

RSC Advances



This is an *Accepted Manuscript*, which has been through the Royal Society of Chemistry peer review process and has been accepted for publication.

Accepted Manuscripts are published online shortly after acceptance, before technical editing, formatting and proof reading. Using this free service, authors can make their results available to the community, in citable form, before we publish the edited article. This *Accepted Manuscript* will be replaced by the edited, formatted and paginated article as soon as this is available.

You can find more information about *Accepted Manuscripts* in the [Information for Authors](#).

Please note that technical editing may introduce minor changes to the text and/or graphics, which may alter content. The journal's standard [Terms & Conditions](#) and the [Ethical guidelines](#) still apply. In no event shall the Royal Society of Chemistry be held responsible for any errors or omissions in this *Accepted Manuscript* or any consequences arising from the use of any information it contains.



Abstract

Tea waste (TW) was modified by depositing hydrated manganese oxide (HMO) onto it through *in situ* precipitation and a novel hybrid bio-adsorbent, namely HMO-TW, was obtained. The successful deposition of HMO in/on tea waste was confirmed by transmission electron microscope (TEM) and Fourier transform infrared spectroscopy (FT-IR) analysis. The removal of four typical heavy metals (i.e., Pb(II), Cd(II), Cu(II), Zn(II)) by HMO-TW was pH-dependent, and higher pH favored the sorption at tested pHs of 2-7. HMO-TW showed excellent sorption selectivity toward all four metal ions, and the removal efficiency of target metal ions sustained at 30%~90% even in the presence of 50 times higher competing Ca(II) and Mg(II) ions. Sorption isotherms of four metal ions by HMO-TW are all well represented by the Freundlich model, and the maximum experimental sorption capacities of Pb(II), Cd(II), Cu(II), Zn(II) were 174.3, 78.38, 54.38 and 37.5 mg g⁻¹, respectively. Compared to the unmodified tea waste, the sorption capacities and selectivity of Pb(II), Cd(II) and Cu(II) onto HMO-TW improved significantly. The sorption process reached equilibrium within 200 min, and the kinetics could be well fitted by a pseudo-second order model. Fixed-bed column sorption results further showed that bed volume (BV) of C_e/C_0 reaching 0.5 for Pb(II), Cd(II), Cu(II), Zn(II) were 1170, 1130, 820 and 1450 BV, respectively. In addition, the exhausted HMO-TW can be effectively regenerated using a 0.5 M HCl solution. All results reported herein validate that HMO-TW is a promising sorbent for practical treatment of heavy metal contaminated water.

40 Introduction

41 Heavy metal contamination has attracted increasing attention due to their high toxicity,
42 widespread presence in many kinds of environmental medium and potential bio-accumulation
43 in food chain.¹ Even at extremely low concentrations, heavy metals can cause many harmful
44 effects towards public health and aquatic life.² Unfortunately, heavy metals are inevitable
45 by-products of rapid economic development. Owing to high perniciousness of heavy metals,
46 stringent regulations have been set up to control their maximum residual concentrations in all
47 industrial effluents of China. For example, Chinese government has set the maximum residual
48 concentrations of Pb(II), Cd(II), Cu(II) and Zn(II) in effluents as 1.0, 0.1, 0.5, and 2.0 mg L⁻¹,
49 respectively.³ Therefore, it is of great importance and urgency to develop efficient and
50 cost-effective technologies for toxic heavy metals removal from wastewater.

51

52 The primary methods for removing heavy metals from water/wastewater include chemical
53 precipitation, adsorption, coagulation, and membrane filtration.^{4,5} Among above-mentioned
54 technologies, adsorption has been generally regarded as one of the most promising
55 technologies.⁶ The development of adsorbent is the key for adsorption technology, and
56 numerous new types of adsorbents like polymer, chelates, and composite have been
57 constantly developed in recent years.⁷⁻¹⁰ Meanwhile, many ordinary and original
58 bio-adsorbents have gradually come into the vision of researchers because of their salient
59 advantages such as easy availability, cheapness and low pollution. For example, wastes like
60 walnut shells,¹¹ tea leaves,¹² rice hulls,¹³ bamboo,¹⁴ corn cobs¹⁵ and eggshell membrane¹⁶⁻¹⁸
61 with reasonable numbers of carboxyl, phenolic hydroxyl and amine groups that can bind to
62 metal ions have been used for toxic metal capture, and some relatively satisfactory results

63 were obtained. Unfortunately, a lot of fatal defects such as low sorption capacity and poor
64 sorption selectivity have seriously limited their further application. The sorption behavior of
65 Pb(II), Cd(II), Cu(II) onto original tea waste (TW) was systematically investigated in our
66 previous research,¹⁹ and the sorption capacities and selectivity of these metals were not very
67 satisfactory. Therefore, it is very imperative to improve the performance of tea waste through
68 some modifications in order to promote its practical application.

69

70 Hydrous manganese oxides (HMO) have always been considered to be one of the most
71 efficacious adsorbents for heavy metal removal due to its specific and strong binding to target
72 metal ion.^{20,21} However, HMO is still far from practical application in fixed-bed and
73 flow-through systems because of excessive pressure drop and difficulty of solid-liquid
74 separation caused by its fine or ultrafine particle size. Some host materials such as activated
75 carbon,^{20,22} zeolite,²³ and porous polymer²⁴ have been selected to synthesize various hybrid
76 adsorbents to overcome this technical barrier and these hybrid sorbents usually have good
77 performance toward heavy metal removal. However, the high cost of these supporting
78 materials makes their application in real world wastewater treatment unaffordable. Therefore,
79 efficient and low-cost supporting materials are still in great demand to facilitate the
80 application of HMO in wastewater treatment.

81

82 In this study, we prepared a novel composite sorbent (HMO-TW) by depositing HMO onto
83 TW to maximally utilize the benefits of both adsorbents for heavy metal removal. We
84 anticipate that TW would be an effective and cost-efficient support for highly dispersed HMO.
85 HMO, on the other hand, provides the composite good selectivity for heavy metal ions against

86 competing cations commonly existing in water (e.g., Ca(II) and Mg(II)). Sorption behaviors
87 of four typical toxic metal ions, Pb(II), Cd(II), Cu(II) and Zn(II), from aqueous solution were
88 investigated by evaluating the influence of solution pH, coexist competing ions, temperature
89 and contact time. Column experiments were performed to simulate the real situation treatment
90 process. In addition, the regeneration of HMO-TW was also evaluated.

91

92 **Experimental**

93 **1. Chemicals**

94 All chemicals used in the current study are analytical grade (AR) or better and were purchased
95 from Guoyao Reagent Station (Anhui, China). Stock solutions containing 1 g L^{-1} of the target
96 heavy metals were prepared by dissolving their corresponding nitrates with ultrapure water
97 (resistivity $> 18.2 \text{ M}\Omega \text{ cm}^{-1}$), which were further diluted prior to use.

98

99 **2. Preparation of HMO-TW**

100 The TW was collected from tea plants located in Green tea region in Huangshan, China. The
101 pretreatment of TW had been described in our previous research.¹⁹ HMO-TW was prepared
102 by in-situ precipitation and the procedures are as following: Firstly, 10.0 g TW after
103 pretreatment was added into $1 \text{ mol L}^{-1} \text{ MnSO}_4 \cdot \text{H}_2\text{O}$ solution and stirred continuously at 303 K
104 for 24 h. Secondly, the Mn(II)-loaded tea waste was filtered from solution and then dried
105 under vacuum at 333 K for 2 h. After this, the solid was added into a binary NaClO-NaOH
106 solution with alkalinity of 10% and active chlorine of 13%, and stirred continuously at 303 K
107 for 24 h to oxidize Mn(II) to Mn(IV) and precipitate.²⁴ Finally, the obtained hybrid materials
108 were washed with 0.1 M HCl and ultrapure water until neutral pH and followed by

109 desiccation under vacuum at 333 K till reaching a constant weight. The final products were
110 stored in sealed glass bottles for future use.

111

112 **3. Batch sorption experiments**

113 Batch sorption experiments were carried out using traditional bottle-point method in 250 mL
114 Erlenmeyer flasks. The detailed experimental information is described in following sections.

115

116 3.1 Effect of solution pH on heavy metal adsorption

117 20.0 mg of HMO-TW particles were dispersed into 100-mL Erlenmeyer flasks containing 50
118 mL solution of either Pb(II) (40 mg L^{-1}), Cd(II) (20 mg L^{-1}), Cu(II) (10 mg L^{-1}) or Zn(II) (10
119 mg L^{-1}). A 1.0 M HCl or NaOH solution was used to adjust the desired solution pH to 2-7
120 throughout the experiments. A thermostatic orbit incubator shaker (New Brunswick Scientific
121 Co. Inc.) was used to shake the stoppered flasks at 120 rpm and 303 K for 24 h, which was
122 sufficient to reach adsorption equilibrium according to preliminary kinetic tests. Finally, the
123 supernatant was sampled and analyzed for equilibrium solution pH and concentration of target
124 metal ions. The amount of adsorbed heavy metals onto HMO-TW was calculated based on
125 mass balance between initial and final metal ion concentrations.

126

127 3.2 Competitive sorption test

128 For the competitive sorption tests, the initial concentrations of heavy metals were 40 mg L^{-1}
129 for Pb(II), 20 mg L^{-1} for Cd(II), 10 mg L^{-1} for Cu(II) and 5 mg L^{-1} of Zn(II), respectively.
130 Other conditions were basically same as the above-mentioned pH effect experiments except
131 certain amount of representative competitive ions (Ca(II) and Mg(II)) were introduced into

132 the test solution.

133

134 3.3 Sorption isotherm

135 For sorption isotherms tests, 20 mg HMO-TW was dispersed into 100 mL flasks containing

136 50 mL solution of various contents of metal ions. The experiment temperature was set at 298

137 K. Langmuir and Freundlich equations ²⁵ were applied to fit the sorption data from the

138 isotherm tests:

$$139 \quad q_e = \frac{K_L q_m C_e}{K_L C_e + 1} \quad (1)$$

$$140 \quad q_e = K_f C_e^{\frac{1}{n}} \quad (2)$$

141 where q_e is the amount of adsorbed metal at equilibrium (mg g^{-1}); C_e is the concentration of

142 the metal ion in solution at equilibrium (mg L^{-1}); q_m is the maximum adsorption capacity of

143 metal on HMO-TW (mg g^{-1}); and K_L (L mg^{-1}) is a binding constant, and both K_f and n are the

144 Freundlich constants.

145

146 3.4 Adsorption kinetics

147 For kinetic tests, 200 mg HMO-TW was added into 1000-mL Erlenmeyer flasks containing

148 500 mL solution of either 70 mg L^{-1} of Pb(II), 25 mg L^{-1} of Cd(II), 30 mg L^{-1} of Cu(II) or 10

149 mg L^{-1} of Zn(II). Aliquots of 0.5 mL were sampled at various time intervals, e.g., every 5 min

150 for 0~30 min, every 10 min for 30~150 min, every 20 min for 150~210 min and every 30 min

151 for 210~360 min. The sorption capacities of heavy metals versus time constituted the kinetic

152 curve.

153

154 The pseudo-second-order equation²⁶ was used to fit the kinetic data:

$$155 \quad q_t = \frac{k_2 q_e^2 t}{tk_2 q_e + 1} \quad (3)$$

156 Where q_e and q_t are sorption capacities of heavy metal (mg g^{-1}) at equilibrium and at time t ,
157 respectively and k_2 is second-order sorption rate constant.

158

159 **4. Fixed-bed column sorption and desorption**

160 In column experiments, a 5-mL aliquot of wet HMO-TW particles was filled into a
161 polyethylene column (12 mm diameter and 130 mm length) equipped with a water bath to
162 maintain a desired temperature. A Lange-580 pump (Baoding, China) was used to ensure a
163 constant flow rate. Simulated wastewater containing given concentration of target metal ions
164 was supplied as influent. A 0.5 M HCl solution was used to regenerate the exhausted
165 HMO-TW after sorption. Detailed operation conditions (e.g., superficial liquid velocity (SLV)
166 and empty bed contact time (EBCT)) are depicted in the related figure captions.

167

168 **5. Analyses**

169 Metal ion concentration in aqueous phase was determined using a TAS-990 flame atom
170 adsorption spectrophotometer (Persee inc., China), and the absorbance of all samples was
171 tested in triplicate. An atom fluorescence spectrophotometer (AF-640) (Ruili Co., Ltd) was
172 also used to determine metal ion content, if lower than 1 mg L^{-1} . The amount of loaded HMO
173 in/on tea waste was calculated using Mn content in aqueous phase after $\text{HNO}_3\text{-HClO}_4$
174 digestion process. FT-IR spectra of HMO-TW before and after metal sorption were obtained
175 using a Nicolet 380 FT-IR spectrometer (USA) with a pellet of powered potassium bromide

176 and adsorbent in the range of 400–4000 cm^{-1} . Speciation of HMO-TW was determined by
177 means of X-ray diffraction analysis with a step size of 0.02° (D8 ADVANCE, Germany). The
178 surface morphology of the host tea waste and HMO-TW was observed using a scanning
179 electron microscope (S-3400N, Japan) and a transmission electron microscopy
180 (JEM-2000EX). The zeta potential of HMO-TW was measured using a Malvern Zetasizer
181 Nano ZS90. N_2 adsorption-desorption tests onto HMO-TW particles were carried out at 77K
182 to obtain specific surface area based on BET model and pore size distribution based on BJH
183 model using a Micromeritics ASAP2020 (USA).

184

185 **Results and discussion**

186 **1. Characterization of the adsorbents**

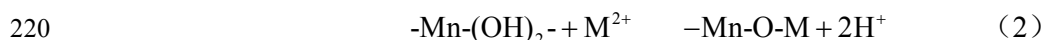
187 The successful deposition of nano-sized HMO particles on the surface of tea waste is clearly
188 shown in a TEM image of HMO-TW (Fig.1a). The sizes of the highly dispersed HMO
189 particles are typically less than 5 nm. The surface morphology of TW was obviously different
190 before and after HMO loading according to SEM images of TW and HMO-TW depicted in
191 Fig.S1. Specifically, the pores located in host tea waste surface were wide and sparse, while
192 the pores became tiny and dense after HMO particles loading. FT-IR spectra of the original
193 tea waste and HMO-TW are depicted in Fig.1b. Obvious sorption peaks of 1623, 915 cm^{-1}
194 assigned to Mn-OH group^{27,28} are observed in the FT-IR spectra of HMO-TW but not TW,
195 which indicates that HMO particles had been successfully loaded onto TW. The zeta potential
196 of HMO-TW (Fig.1c) was always negative in the tested pH range of 2-10, indicating
197 HMO-TW can strongly attract cations. The broad and weak diffraction peaks in X-ray
198 diffraction pattern of HMO-TW (Fig.S2) are similar to those of $\delta\text{-MnO}_2$,²⁹ which suggests

199 that most of the loaded HMO is amorphous in nature. Some major physicochemical properties
 200 of the host TW and HMO-TW are listed in Table 1. The loaded HMO amount on TW was
 201 4.82(w/w)% in Mn mass, while no Mn was detected in the supporting TW. The larger BET
 202 specific surface area of HMO-TW ($5.92 \text{ m}^2 \text{ g}^{-1}$) compared to that of host TW ($0.86 \text{ m}^2 \text{ g}^{-1}$)
 203 should result from the large surface area of HMO, which was reported to be $100.5 \text{ m}^2 \text{ g}^{-1}$ ²⁸
 204 (Note that the HMO content is only 4.86% as Mn in HMO-TW).

205

206 2. Effect of Solution pH

207 Solution pH is a significant environmental factor that usually influences the sorption process
 208 by altering surface properties of the sorbent and the speciation of the sorbate. Therefore,
 209 removal of Pb(II), Cd(II), Cu(II) and Zn(II) by HMO-TW at different solution pH was
 210 conducted, and the effect curves are shown in Fig. 2. The removal efficiency of heavy metals
 211 increased with the increase of solution pH. More specifically, the removal of heavy metals
 212 almost linearly increased at acidic pH range 2-5, and became more gradual at the near neutral
 213 pH range 5-7. The above pH effect results are consistent to sorption of many heavy metals
 214 onto other adsorbents,^{15,28,30} which can be explained by the exchange of H in functional
 215 groups of sorbent with target metal ions. In our previous research, we elucidated the ion
 216 exchange process between the functional groups, e.g. carboxyl and phenolic hydroxyl groups,
 217 on TW and the target metal ions.¹⁹ For the as-prepared HMO-TW, the loaded HMO would
 218 result in the same pH effect by forming inner-sphere complexes with metal ions as ^{31,32}



221 Obviously, more H^+ , namely, lower solution pH, is unfavorable for heavy metals sorption

222 onto loaded HMO, while higher pH promotes the above reactions. The inner-sphere
223 complexes between Mn-OH and heavy metals had been extensively researched previously
224 using EXAFS.^{33,34} The combined effects of HMO and host TW lead to the pH-dependent
225 plots depicted in Fig. 2. Besides, the contents of Mn released into solution after Pb(II)
226 adsorption at different pHs (2-7) were analyzed, and no Mn leaching was detected (data not
227 shown). Thus, HMO-TW could be an ideal sorbent for heavy metals removal from slightly
228 acidic wastewater (e.g., pH 4-7) in terms of both material stability and removal performance.

229

230 3. Effect of coexisting ions

231 The effects of co-existing alkali and alkaline-earth metal cations on Pb(II), Cd(II), Cu(II) and
232 Zn(II) adsorption by HMO-TW were conducted, and the results are shown in Fig.3. Here, two
233 divalent cations with low hydration energy, Ca(II) ($-1656 \text{ KJ mol}^{-1}$) and Mg(II) (-2049 KJ
234 mol^{-1}),³⁵ were selected as representative co-ions because of their stronger competition for
235 heavy metal adsorption than Na(I) or K(I). The addition of Ca(II) and Mg(II) resulted in
236 decline of the sorption of four heavy metals onto HMO-TW to various degrees. Specifically,
237 only slight drop of removal efficiency ($< 25\%$) (i.e., good selectivity) was observed for
238 Pb(II) and Cu(II) in the presence of co-ions with 0 to 50 times higher concentrations.
239 However, greater impacts with drop of removal efficiency up to 60% were observed for Cd(II)
240 and Zn(II).

241

242 The sorption selectivity order of Pb(II)>Cd(II)>Zn(II) can be explained using two
243 mechanisms, ion exchange with the host TW and inner-sphere complexes with the loaded
244 HMO. Generally, the hydration energy of metal ions is related to their ion exchange ability,

245 and lower hydration energy favors ion exchange.³⁶ Thus, Pb(II) with lower hydration energy
246 (-1504 KJ mol⁻¹) compared to that of Cd(II) (-1708 KJ mol⁻¹) and Zn(II) (-1992 KJ mol⁻¹)³⁵
247 had the most ion exchange with TW. As for the inner-sphere complexes with HMO, it can be
248 illustrated by the hard and soft acids and bases (HSAB) principle.³⁷ Here, the target heavy
249 metal ions act as Lewis acids while HMO as a Lewis base. We note that the softness of Pb(II)
250 is higher than that of Cd(II) and Zn(II) as a result of their different ionic radius (0.118 nm for
251 Pb(II), 0.095 nm for Cd(II) and 0.075 nm for Zn(II)). Since high softness favors Lewis
252 acid-base interaction, the adsorption of Pb(II) to HMO was the strongest (i.e., best
253 selectivity).

254

255 The stronger adsorption selectivity of Cu(II) than Cd(II) and Zn(II) is somewhat unexpected
256 since Cu(II) has the highest hydration energy (-2030 KJ mol⁻¹) and the smallest ionic radius
257 (0.073 nm), which suggest the lowest ion exchange and weakest HMO-Cu(II) interaction. The
258 results can be attributed to the amine groups on host TW, which form strong, specific
259 coordination with Cu(II).^{38, 39} This also explains that the sorption of Cu(II) onto TW was
260 higher than Cd(II) although Cu(II) has much higher hydration energy in our previous study.¹⁹

261

262 Since TW does not have satisfactory selectivity for metal ion adsorption, the good sorption
263 selectivity of HMO-TW is mainly from the HMO on TW, which is known to have strong
264 sorption specificity for heavy metals. Nonetheless, the functional group rich TW can facilitate
265 the sorption selectivity through the Donnan membrane effect⁴⁰ caused by the attraction of
266 positively charge metal ions by non-diffusible, negatively charged carboxyl groups on TW.
267 The Donnan membrane effect is illustrated in [Fig.S3](#). The Ca(II) had greater influence than

268 Mg(II) on sorption of all four heavy metals by HMO-TW as expected due to its lower Gibbs
269 free energy of hydration.³⁶

270

271 The distribution coefficient K_d (L g⁻¹) is also introduced to quantify the sorption selectivity of
272 four metal ions onto HMO-TW⁴¹

$$273 \quad K_d = \frac{C_o - C_e}{C_e} \times \frac{V}{m} \quad (3)$$

274 Where C_o (mg L⁻¹) is the aqueous initial heavy metal ion concentration, C_e is the aqueous
275 heavy metal ion concentration at equilibrium (mg L⁻¹), V (mL) is the volume of the solution,
276 and m (g) is the mass of the adsorbent. Table 2 summarized the K_d values for four heavy metal
277 ions in the presence of different levels of Ca(II) and Mg(II). The trend of K_d value variation is
278 in good agreement with the curves in Fig. 3.

279

280 Sorption Isotherms and Kinetic

281 The sorption isotherms of Pb(II), Cd(II), Cu(II) and Zn(II) by HMO-TW were investigated at
282 298K, and the results are illustrated in Fig. 4. The sorption capacities of four metal ions all
283 increased with the increase of C_e as well as C_o (Fig.S4). Subsequently, the four isotherms are
284 fitted using both the Freundlich and Langmuir models. Generally, the Langmuir model refers
285 to a monolayer adsorption onto homogeneous surface with no interactions between the
286 adsorbed molecules, and the Freundlich model is an empirical equation usually used to
287 describe chemisorption on heterogeneous surface sorption.⁴² The detailed fitted parameters are
288 listed in Table 3. As shown, the sorption isotherms of four heavy metals can be better fitted
289 by the Freundlich model than the Langmuir one, with related coefficients R^2 larger than 0.962.
290 The better fitting of Freundlich model indicates a chemisorption process, and the effective

291 binding sites on HMO-TW surface for four metal ions are heterogeneous. The strong
292 interaction (e.g., inner-sphere complexes) between heavy metal ions and HMO clearly
293 contributes to the heterogeneous chemisorption process. The experimental sorption capacities
294 for Pb(II), Cd(II), Cu(II) and Zn(II) were 174.3, 78.38, 54.38 and 37.5 mg g⁻¹, respectively.
295 The capacities for Pb(II), Cd(II) and Cu(II) are much higher than the calculated q_m values of
296 the host TW, which were 26.98 mg g⁻¹ for Pb(II), 15.04 mg g⁻¹ for Cd(II) and 18.54 mg g⁻¹ for
297 Cu(II).¹⁹

298

299 It is worth noting that the utilization efficiency of unit mass Mn is improved for around 5
300 times by loading HMO onto tea waste. The Pb(II), Cd(II) and Zn(II) sorption capacities of
301 unit mass Mn for HMO-TW were 3616.2, 1626.1 and 778 mg g⁻¹, respectively, and for pure
302 HMO were 710.1, 304.1 and 117.7 mg g⁻¹, respectively.²⁸ The improvement of Mn utilization
303 efficiency can be attributed to the dispersion of HMO nanoparticles (< 5nm based on TEM)
304 on TW increased accessible binding sites of HMO. In addition, the sorption capacities of
305 Pb(II), Cd(II), Cu(II) and Zn(II) by HMO-TW and other previously reported materials are
306 compared in Table 5. The sorption capacities of four heavy metals onto HMO-TW are better
307 than most previously reported sorbents with low-cost merits. It is also noteworthy that
308 HMO-TW is more applicable for heavy metal removal from lightly polluted water base on the
309 results depicted in Fig.S4. The removal efficiency of four toxic metals decreased with the
310 increase of initial metal ion concentration, which can be explained by the diminished
311 opportunities of target metal ions binding to sorption sites on HMO-TW at higher initial
312 concentrations.

313

314 The sorption kinetics of the four heavy metal ions onto HMO-TW was also investigated (Fig.
315 5). The sorption process was very quick by HMO-TW in the initial 100 min then slowed
316 down to approach sorption equilibrium within 200 min. The kinetic data of all heavy metal
317 ions were well fitted by the pseudo-second-order model, and the fitting parameters are listed
318 in Table 4. The calculated q_e values based on pseudo-second-order model (110.3 mg g⁻¹ for
319 Pb(II), 37.7 mg g⁻¹ for Cd(II), 28.2 mg g⁻¹ for Cu(II), 17.3 mg g⁻¹ for Zn(II)) are close to the
320 experimental data (119.28 mg g⁻¹ for Pb(II), 38.45 mg g⁻¹ for Cd(II), 29.35 mg g⁻¹ for Cu(II),
321 18.03 mg g⁻¹ for Zn(II)). The sorption of heavy metal ions by HMO-TW was relatively slow
322 compared to host TW, which may be caused by the pore blockage effect as a result of HMO
323 loading.

324

325 **Fix-bed Column Sorption and regeneration**

326 Fix-bed column sorption trail is an essential step for evaluating the engineering application
327 potential of a given sorbent. The column sorption tests of HMO-TW were conducted, and the
328 complete effluent history is described in Fig. 6. The bed volume (BV) of C_e/C_0 reaching 0.5
329 for Pb(II), Cd(II), Cu(II) and Zn(II) are around 1170, 1130, 820 and 1450 BV, respectively.
330 Note that almost no target heavy metal ions was detected in the effluent until a sudden
331 increase after 830 BV for Pb(II), 400 BV for Cd(II), 650 BV for Cu(II) and 950 BV for Zn(II).
332 The excellent results of all four heavy metal adsorption by HMO-TW in the column tests,
333 especially in the early stage, imply that HMO-TW has great potential for practical wastewater
334 treatment in flow-through systems.

335

336 The exhausted HMO-TW was able to be regenerated using a 0.5 M HCl solution at 298 K as

337 shown in Fig. 7. The adsorbed heavy metals were completely regenerated after only 6-BV of
338 HCl solution flushing, and the regeneration efficiency was larger than 95%. In addition, only
339 negligible Mn was detected in the regeneration solution.

340

341 **Conclusions**

342 A novel bio-adsorbent HMO-TW was successfully prepared by impregnating hydrated
343 manganese oxide (HMO) onto tea waste. Sorption of Pb(II), Cd(II), Cu(II) and Zn(II) onto
344 HMO-TW was observed to be pH-dependent due to a combined effect induced by the
345 ion-exchange with the host TW and the inner-sphere complexation with impregnated HMO.
346 Even in the presence of competing ions with 50 times higher concentration, HMO-TW
347 maintained excellent sorption selectivity toward four heavy metal ions due to the specific
348 binding between heavy metal ions and the loaded HMO and Donnan membrane effect.
349 Besides, the sorption of four metal ions onto HMO-TW can be well fitted by the Freundlich
350 model and a pseudo-second-order model. Satisfactory results of column sorption and
351 regeneration tests further show that HMO-TW is a promising sorbent for removing heavy
352 metals from contaminated water in engineering settings.

353

354 **Acknowledgement**

355 This work has been supported by the Science Foundation for Excellent Youth Scholars of
356 Universities and Colleges of Anhui Province (2013SQRL091ZD), Innovative Training of
357 College Students of Huangshan University (AH2014103753123) and the National Natural
358 Science Foundation of China (No. 51308312).

359

360 **References**

- 361 1 C. Cheng, J.N.Wang, X. Yang, A.M.Li and C.Philippe, *J. Hazard. Mater.*, 2014, **264**, 332-341.
- 362 2 N. Isobe, X. Chen, U. Kim, S. Kimura, M. Wada, T. Saito and A. Isogai, *J. Hazard. Mater.*, 2013,
363 **260**, 195-201.
- 364 3 China MEP (Ministry of environmental protection), Integrated wastewater discharge standard
365 (GB8798-1996), 1996.
- 366 4 M. Hua, S. Zhang, B. Pan, W. Zhang, L. Lv and Q. Zhang, *J. Hazard. Mater.*, 2012, **211–212**,
367 317-331.
- 368 5 Y. Zhang, Y. N. Chen, C. Z. Wang and Y. M. Wei, *J. Hazard. Mater.*, 2014, **276**, 129-137.
- 369 6 P. Tan, J. Sun, Y. Y. Hu, Z. Fang, Q. Bi, Y. C. Chen, J. H. Cheng, *J. Hazard. Mater.*, 2015, **297**,
370 251-260.
- 371 7 L. D. Pablo, M. L. Chávez and M. Abatal, *Chem. Eng. J.*, 2011, **171**, 1276-1286.
- 372 8 D. Kołodynska, M. Kowalczyk, Z. Hubicki, V. Shvets and V. Golub, *Chem. Eng. J.*, 2015, **276**,
373 376-387.
- 374 9 L. C. Lin and R.S.Juang, *Chem. Eng. J.*, 2005, **112**, 211-218.
- 375 10 C. Shan, Z. Y. Ma, M. P. Tong and J. R. Ni, *Water Res.*, 2015, **69**, 252-260.
- 376 11 T. Altun and E. Pehlivan, *Food Chem.*, 2012, **132**, 693-700.
- 377 12 S. K. Prabhakaran, K. Vijayaraghavan and R. Balasubramanian, *Ind. Eng. Chem. Res.*, 2009, **48**,
378 2113-2117.
- 379 13 N. Gupta, S. S. Amritphale and N. Chandra, *Bioresour. Technol.*, 2010, **101**, 3355-3362.
- 380 14 X. O. Yang, R. N. Jin, L. P. Yang, Z. S. Wen, L. Y. Yang, Y. G. Wang, and C. Y. Wang, *J. Agric.*
381 *Food Chem.*, 2014, **62**, 6007-6015.
- 382 15 M. Sciban, M. Klasnja and B. Skrbic, *Desalination*, 2008, **229**,170-180.
- 383 16 S. Wang, M.H. Wei and Y.M. Huang, *J. Agric. Food Chem.*, 2013, **61**, 4988-4996.
- 384 17 W.T. Tsai, J.M. Yang, C.W. Lai, Y.H. Cheng, C.C. Lin and C.W. Yeh, *Bioresour. Technol.*, 2006,
385 **97**, 488–493.
- 386 18 B. Liu and Y. M. Huang, *J. Mater. Chem.*, 2011, **21**, 17413-17418.
- 387 19 S. Wan, Z. Ma, Y. Xue, M. Ma, S. Xu, L. Qian and Q. Zhang, *Ind. Eng. Chem. Res.*, 2014, **53**,
388 3629-3635.
- 389 20 H. J. Fan and P. R. Anderson, *Sep. Purif. Technol.*, 2005, **45**, 61-67.

- 390 21 S. S. Tripathy, J. L. Bersillon and K. Gopal, *Desalination*, 2006, **194**, 11-21.
- 391 22 S. M. Lalhmunsiam and L. D. Tiwari, *Chem. Eng. J.*, 2013, **225**, 128-137.
- 392 23 R. P. Han, W. H. Zou, H. K. Li, Y. H. Li and J. Shi, *J. Hazard. Mater.*, 2006, **137**, 934-942.
- 393 24 Q. Su, B. C. Pan, B. J. Pan, Q. R. Zhang, W. M. Zhang, L. Lv, X. S. Wang, J. Wu and Q. X. Zhang,
394 *Sci. Total Environ.*, 2009, **407**, 5471-5477.
- 395 25 C. H. Giles, D. Smith and A. Huitson, *J. Colloid Interface Sci.*, 1974, **47**, 755-765.
- 396 26 Y. S. Ho and G. McKay, *Water Res.*, 2000, **34**, 735-742.
- 397 27 M. V. Ananth, S. Pethkar and K. Dakshinaurthi, *J. Power Sour.*, 1998, **75**, 278-282.
- 398 28 Q. Su, B.C. Pan, S.L. Wan, W.M. Zhang and L. Lv, *J. Colloid Interface Sci.*, 2010, **349**, 607-612.
- 399 29 B. J. Lafferty, M. Ginder-Vogel, M. Q. Zhu, K. J. T. Livi and D. L. Sparks, *Environ. Sci. Technol.*,
400 2010, **44**, 8467-8472.
- 401 30 X. Y. Guo, B. Du, Q. Wei, J. Yang, LH. Hu, L. G. Yan and W. Y. Xu, *J. Hazard. Mater.*, 2014, **278**,
402 211-220.
- 403 31 S. B. Kanungo, S. B. Tripathy and S. K. Mishra, *J. Colloid Interface Sci.*, 2004, **269**, 11-21.
- 404 32 H. Tamura, N. Katayama and R. Furuichi, *Environ. Sci. Technol.*, 1996, **30**, 1198-1204.
- 405 33 L. Bochatay, P. Persson and S. Sjoberg, *J. Colloid Interf. Sci.*, 2000, **229**, 584-592.
- 406 34 L. Bochatay and P. Persson, *J. Colloid Interf. Sci.*, 2000, **229**, 593-599.
- 407 35 Y. Marcus, *J. Chem. Soc. Faraday Trans.*, 1991, **87**, 2995-2999.
- 408 36 M. M. Abou-Mesalam, *Colloids Surf. A.*, 2003, **225**, 85-94.
- 409 37 M. Misono, E. Ochiai, Y. Saito and Y. Yoneda, *J. Inorg. Nucl. Chem.*, 1967, **29**, 2685-2691.
- 410 38 D. R. Chang, S. Harden and N. Loverro, *J. Macromol. Sci., Part A: Pure Appl. Chem.*, 1986, **23**,
411 801-804.
- 412 39 Y. L. Chen, B. C. Pan, H. Y. Li, W. M. Zhang, L. Lv and J. Wu, *Environ. Sci. Technol.*, 2010, **44**,
413 3508-3513.
- 414 40 L. Cumbal and A. K. Sengupta, *Environ. Sci. Technol.*, 2005, **39**, 6508-6515.
- 415 41 Q. R. Zhang, Q. Du, T. Jiao, B. Pan, Z. Zhang, Q. Sun, S. Wang, T. Wang, F. Gao, *Chem. Eng. J.*,
416 2013, **221**, 315-321.
- 417 42 M. Zhang, B. Gao, S. Varnosfaderani, A. Hebard, Y. Yao and M. Inyang, *Bioresour. Technol.*,
418 2013, **130**, 457-462.
- 419 43 M.A. Farajzadeh and A.B. Monji, *Sep. Purif. Technol.*, 2004, **138**, 197-207.

- 420 44 P. Wang, M. L. Du, H. Zhu, S. Y. Bao, T. T. Yang and M. L. Zou, *J. Hazard. Mater.*, 2015, **286**,
421 533-544.
- 422 45 S. G. Wang, W. X. Gong, X. W. Liu, Y. W. Yao, B. Y. Gao and Q. Y. Yue, *Sep. Purif. Technol.*, 2007,
423 **58**, 17-23.
- 424 46 R. P. Han, Z. Lu, W. H. Zou, D. T. Wang, J. Shi and J. Yang, *J. Hazard. Mater.*, 2006, **B137**,
425 480-488.
- 426 47 E. Pehlivan and T. Altun, *J. Hazard. Mater.*, 2007, **140**, 299-307.
- 427 48 P. Tan, J. Sun, Y. Y. Hu, Z. Fang, Q. Bi, Y. C. Chen and J. H. Cheng, *J. Hazard. Mater.*, 2015, **297**,
428 251-260.
- 429 49 J. E. Ramiro, R. P. Martinsa and A. R. R. Boaventura, *Water Res.*, 2004, **38**, 693-699.
- 430 50 R. Zhao, X. Li, B. Sun, M. Shen, X. Tan, Y. Ding, Z. Jiang and C. Wang, *Chem. Eng. J.*, 2015, **268**,
431 290-299.
- 432 51 Y.S. Ho, C.T. Huang and H.W. Huang, *Process Biochem.*, 2002, **37**, 1421-1430.
- 433

434 Table 1 Major physicochemical properties of the host tea waste and HMO-TW

| Designation | Tea waste | HMO-TW |
|--|-------------------------------|---------------------------------------|
| Functional group | -COOH, -NH ₂ , -OH | -COOH, -NH ₂ , -OH and HMO |
| Particles size (mm) | 0.25~0.88 | 0.25~0.88 |
| BET surface area (m ² g ⁻¹) | 0.86 | 5.92 |
| Average pore diameter (nm) | 3.62 | 1.03 |
| Mn content (%) | 0 | 4.82 |

435

436 Table 2 Distribution coefficients (K_d) of Pb(II), Cd(II), Cu(II) and Zn(II) for HMO-TW in the
437 presence of different levels of Ca(II) and Mg(II)

438

| Competing ions | Heavy metals | K_d (mL g ⁻¹) at different initial Ca(II) or Mg(II)/M(II) ratios in solution (mol/mol) | | | | |
|----------------|--------------|--|-------|-------|-------|-------|
| | | 5 | 10 | 15 | 20 | 50 |
| Ca(II) | Pb(II) | 23644 | 25048 | 16105 | 15967 | 12260 |
| | Cd(II) | 4799 | 3263 | 2589 | 2024 | 1224 |
| | Cu(II) | 15681 | 14167 | 8968 | 8661 | 5325 |
| | Zn(II) | 4238 | 2935 | 2336 | 1737 | 1400 |
| Mg(II) | Pb(II) | 30126 | 24418 | 18959 | 15013 | 73039 |
| | Cd(II) | 11105 | 4122 | 3616 | 2628 | 1468 |
| | Cu(II) | 26740 | 18333 | 12293 | 12652 | 8736 |
| | Zn(II) | 13028 | 6241 | 6091 | 5751 | 3221 |

439

440

441 Table 3 Isotherm constants for uptakes of Pb(II), Cd(II), Cu(II) and Zn(II) onto HMO-TW
 442 at 298K

| Heavy metals | Freundlich model | | | Langmuir model | | |
|--------------|--|------|-------|--------------------------|--------------------------|-------|
| | $K_f (\text{mg}^{1-n} \text{L}^n \text{g}^{-1})$ | n | R^2 | $K_L (\text{L mg}^{-1})$ | $q_m (\text{mg g}^{-1})$ | R^2 |
| Pb(II) | 101.18 | 0.17 | 0.974 | 0.99 | 172.50 | 0.882 |
| Cd(II) | 47.19 | 0.13 | 0.979 | 1.55 | 72.88 | 0.807 |
| Cu(II) | 28.15 | 0.19 | 0.962 | 1.08 | 52.70 | 0.887 |
| Zn(II) | 19.92 | 0.16 | 0.988 | 3.27 | 32.37 | 0.756 |

443

444

445

Table 4 Kinetic parameters of Pb(II), Cd(II), Cu(II) and Zn(II) removal by HMO-TW at 298
 K

| Heavy metals | Pseudo-second-order | | | Experimental values |
|--------------|---------------------------------|--------------------------|-------|--------------------------|
| | $k_2, 10^{-2} \text{ min}^{-1}$ | $q_e, \text{ mg g}^{-1}$ | R^2 | $q_e, \text{ mg g}^{-1}$ |
| Pb(II) | 1.80 | 110.3 | 0.957 | 118.9 |
| Cd(II) | 1.41 | 37.7 | 0.994 | 38.4 |
| Cu(II) | 2.38 | 28.2 | 0.991 | 29.0 |
| Zn(II) | 1.00 | 17.3 | 0.993 | 18.0 |

446

447

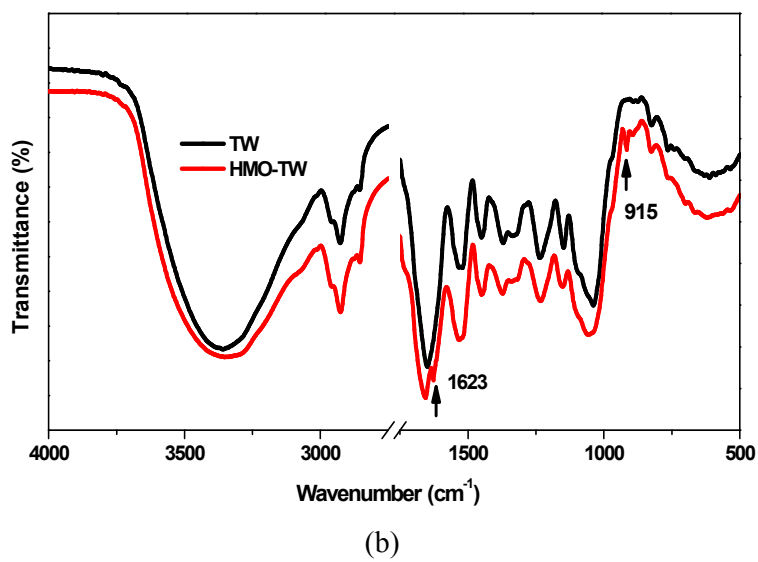
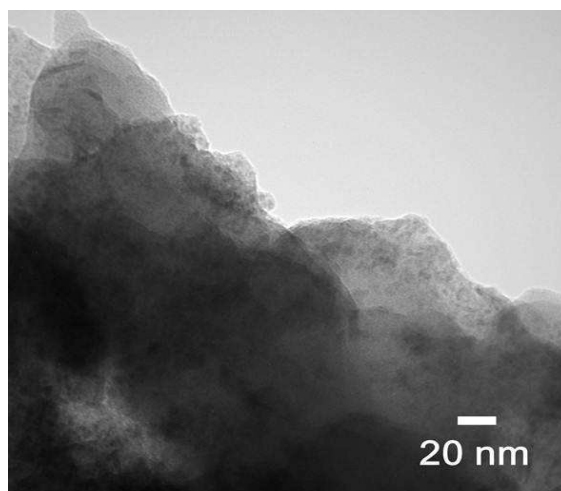
448 Table 5 Comparison of the sorption capacities for Pb(II), Cd(II), Cu(II) and Zn(II) onto
 449 various adsorbents

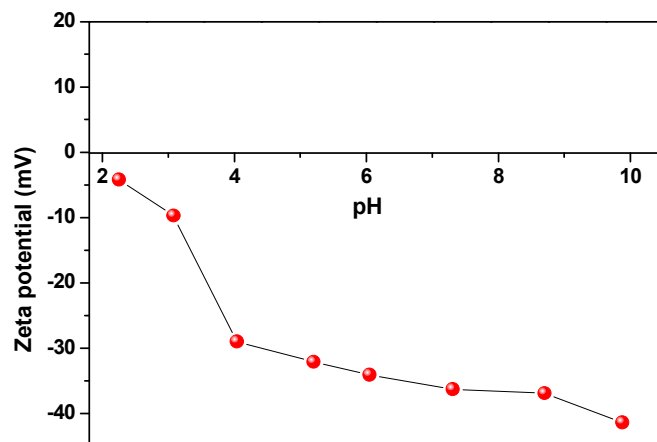
| Sorbent | Metal ions | Conditions | Sorption capacity (mg g ⁻¹) | Refs. |
|--|------------|--------------|--|---------------|
| HMO-TW | Pb(II) | pH 5.5 298 K | 174.3 | Present study |
| The host tea waste | Pb(II) | pH 5.0 298 K | 33.49 | 19 |
| Wheat bran | Pb(II) | NA | 63.9 | 43 |
| SD-SNTs | Pb(II) | pH 7.0 303 K | 112.36 | 44 |
| HMO-D001 | Pb(II) | pH4.4 298 K | 395 | 24 |
| Manganese oxide-coated carbon nanotubes | Pb(II) | pH 5.0 323 K | 78.74 | 45 |
| manganese oxide coated sand | Pb(II) | pH 4.0 318 K | 1.9 | 46 |
| HMO-TW | Pb(II) | pH 5.5 298 K | 78.38 | Present study |
| The host tea waste | Cd(II) | pH 5.5 298 K | 15.04 | 19 |
| Wheat bran | Cd(II) | NA | 24.2 | 43 |
| Lewatit CNP 80 | Cd(II) | pH 8 298 K | 4.48 | 47 |
| Graphene oxide membranes | Cd(II) | pH 5.8 303 K | 83.8 | 48 |
| Moss | Cd(II) | pH 5.0 303 K | 29.0 | 49 |
| Phosphorylated PAN-based nanofiber | Cd(II) | NA | 37.3 | 50 |
| HMO-TW | Cd(II) | pH 5.5 298 K | 54.38 | Present study |
| The host tea waste | Cu(II) | pH 5.0 298 K | 18.54 | 19 |
| Wheat bran | Cu(II) | NA | 14.5 | 43 |
| Graphene oxide membranes | Cu(II) | pH 5.8 303 K | 72.6 | 48 |
| manganese oxide coated sand | Cu(II) | pH 4.0 318 K | 0.48 | 46 |
| Lewatit CNP 80 | Cu(II) | pH 8 298 K | 10.24 | 47 |
| HMO-TW | Zn(II) | pH 5.5 298 K | 37.5 | Present study |
| Moss | Zn(II) | pH 5.0 303 K | 15.0 | 49 |
| Lewatit CNP 80 | Zn(II) | pH 8 298 K | 20.15 | 47 |
| Tree fern | Zn(II) | NA | 7.58 | 51 |

450 NA: not available

451

452 Fig.1 Physical characterization of TW and HMO-TW: (a) TEM of HMO-TW; (b) FT-IR
453 spectrum of TW and HMO-TW; and (c) Zeta potential of HMO-TW at 298 K.
454





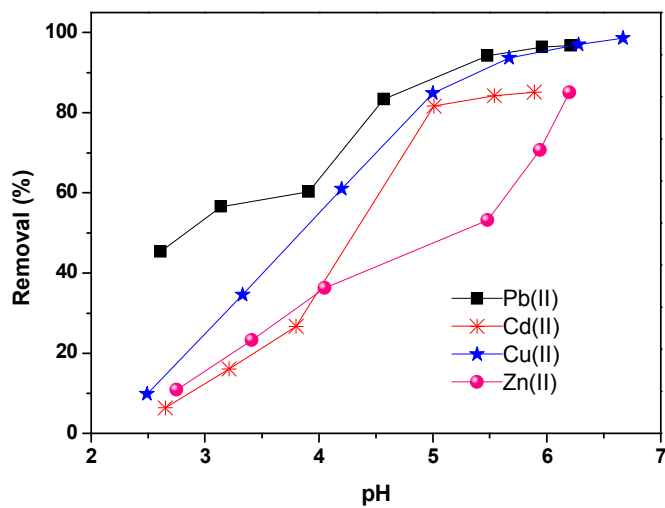
460

461

462

(c)

463 Fig.2 Influence of pH on sorption of Pb(II), Cd(II), Cu(II) and Zn(II) by HMO-TW.
464 Conditions: C_0 (Pb(II)) = 40 mg L⁻¹; C_0 (Cd(II)) = 20 mg L⁻¹; C_0 (Cu(II)) = 10 mg L⁻¹; C_0
465 (Zn(II)) = 10 mg L⁻¹; sorbent dose = 0.4 g L⁻¹; Temperature = 298 K.

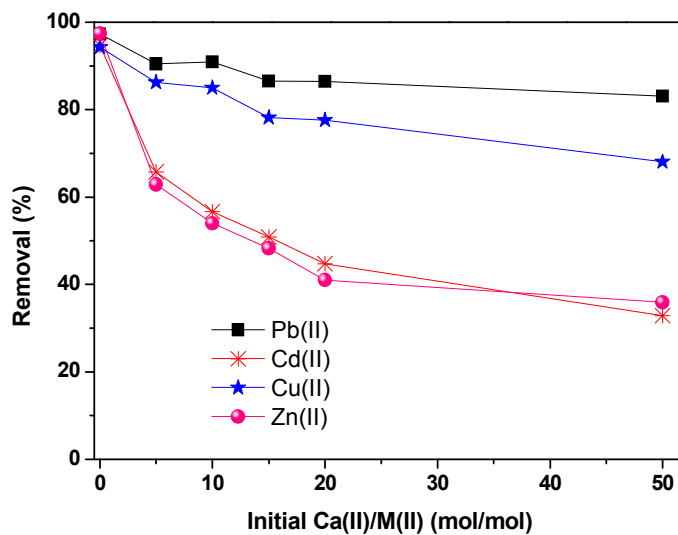


466

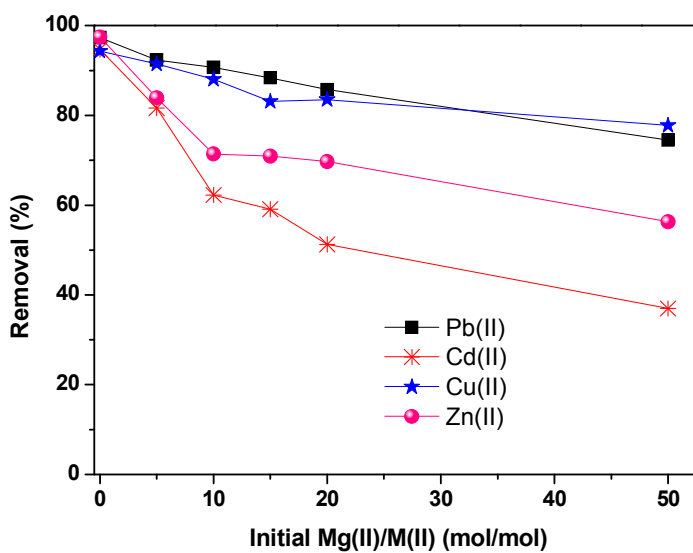
467

468

469 Fig. 3 Influence of Ca(II) (a) and Mg(II) (b) on sorption of Pb(II), Cd(II), Cu(II) and Zn(II) by
470 HMO-TW. Conditions: C_0 (Pb(II)) = 40 mg L⁻¹; C_0 (Cd(II)) = 20 mg L⁻¹; C_0 (Cu(II)) = 10 mg
471 L⁻¹; C_0 (Zn(II)) = 5 mg L⁻¹; sorbent dose = 0.4 g L⁻¹; pH = 5.5±0.2; Temperature = 298 K.



(a)

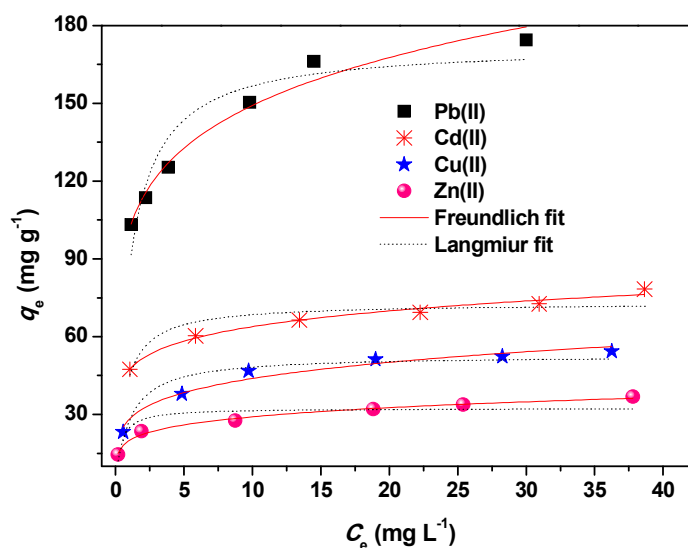


(b)

472
473
474

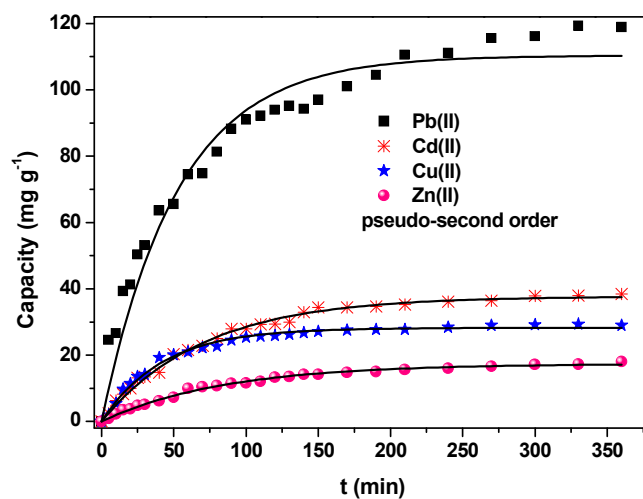
475
476
477
478
479

480 Fig. 4 Sorption isotherms of Pb(II), Cd(II), Cu(II) and Zn(II) onto HMO-TW. Conditions:
 481 Sorbent dose = 0.4 g L⁻¹; pH = 5.5±0.2; Temperature = 298 K.
 482



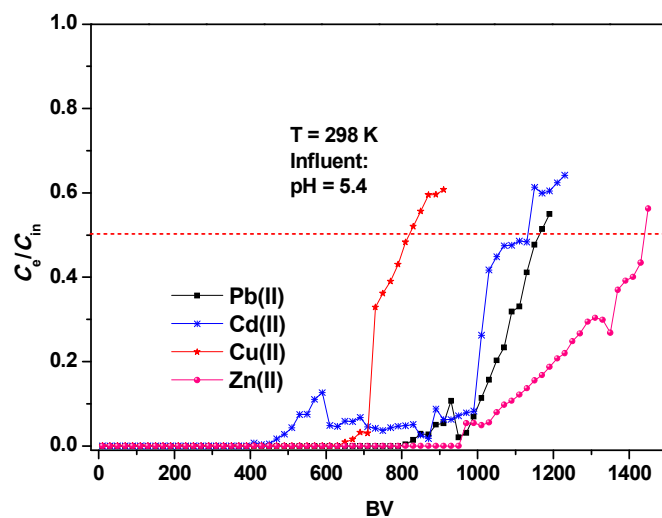
483
 484

485 Fig.5 Sorption kinetics of Pb(II), Cd(II), Cu(II) and Zn(II) onto HMO-TW. Conditions: C₀
 486 (Pb(II)) = 70 mg L⁻¹; C₀ (Cd(II)) = 25 mg L⁻¹; C₀ (Cu(II)) = 30 mg L⁻¹; C₀ (Zn(II)) = 10 mg
 487 L⁻¹; sorbent dose = 0.4 g L⁻¹; pH = 5.5±0.2; Temperature = 298 K.



488
 489

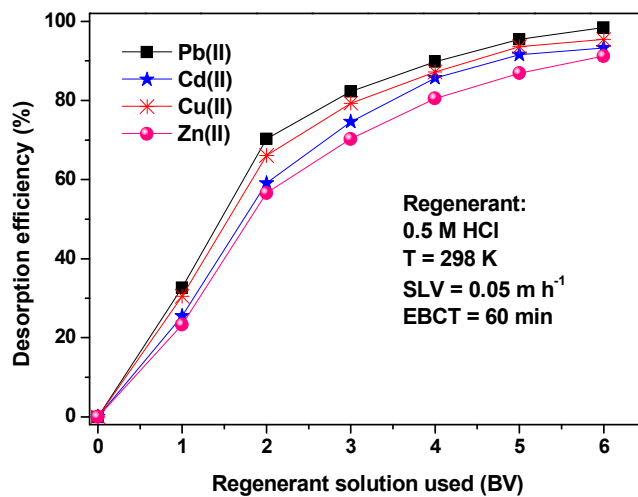
490 Fig. 6 Breakthrough curves of Pb(II), Cd(II), Cu(II) and Zn(II) in a column system filled with
491 5 mL wet HMO-TW. Conditions: Influent concentration (C_{in}) of Pb(II) = 9.0 mg L⁻¹; C_{in}
492 (Cd(II)) = 1.5 mg L⁻¹; C_{in} (Cu(II)) = 2.7 mg L⁻¹; C_{in} (Zn(II)) = 1.1 mg L⁻¹.



493

494

495 Fig. 7 The cumulative desorption curves of the exhausted HMO-TW in column flushed with
496 0.5 M HCl.



497